



## Research article

## Kinetic estimation of solid state transition during isothermal and grinding processes among efavirenz polymorphs

Yoga Windhu Wardhana<sup>a,b,\*</sup>, Arie Hardian<sup>c,e</sup>, Anis Y. Chaerunisa<sup>b</sup>, Veinardi Suendo<sup>c,d</sup>, Sundani N. Soewandhi<sup>a,d</sup><sup>a</sup> Department of Pharmaceutics, School of Pharmacy, Institute Technology of Bandung (ITB), Indonesia<sup>b</sup> Department of Pharmaceutics and Pharmaceuticals Technology, Faculty of Pharmacy, Universitas Padjadjaran (UNPAD), Indonesia<sup>c</sup> Inorganic and Physical Chemistry Division, Faculty of Mathematics and Natural Sciences, ITB, Indonesia<sup>d</sup> Research Center for Nanoscience and Nanotechnology, Institute Technology of Bandung (ITB), Indonesia<sup>e</sup> Department of Chemistry, Faculty of Mathematics and Natural Sciences, University of Jenderal Achmad Yani (UNJANI), Indonesia

## ARTICLE INFO

## Keywords:

Efavirenz  
Bimorphism  
Rietveld refinement  
Isothermal  
Grinding  
Kinetics study  
Materials characterization  
Materials chemistry  
Materials processing  
Materials structure  
Physical chemistry  
Pharmaceutical chemistry

## ABSTRACT

Investigation into the solid-state transition among drug polymorphs has been more intense lately. Many factors induce the transformation of polymorphs during manufacturing processes. Efavirenz (EFV), an AIDS therapy drug, has more than 23 polymorphs, but very little information has been reported on them. This study aimed to perform a characterisation of EFV polymorph properties and to predict the kinetics and mechanism of the polymorphic transformation of EFV during manufacturing processes. The bimorphism study was conducted by Differential Scanning Calorimetry (DSC) thermal analysis. The phase transition kinetics of the polymorphs was monitored by X-ray powder diffraction and the quantification of concomitant polymorphs was examined using Rietveld refinement with MAUD ver. 2.7 as a software aid. To predict the solid-state transition, correlation coefficients of solid-state kinetic models were fitted to the experimental data. The results show that Form I and Form II of EFV were thermodynamically shown to be monotropy related. By fitting the experimental data, it was found that isothermal treatment had the best model fit with the phase boundary reaction in the two-dimensional model (G2). Accordingly, by employing mechanical treatment (grinding), it was predicted that the transition mechanism is a second-ordered reaction (R2). The activation energy of the transition during isothermal treatment calculated by the Arrhenius plot was found to be 23.051 kJ mol<sup>-1</sup>; the half-life of Form II at ambient temperature was 428.05 min (~7.1 h).

## 1. Introduction

The polymorphism phenomenon in drug substances has been the subject of investigation in pharmaceutical development for many years. The polymorphs of an active pharmaceutical compound may have different crystal forms or distinct structures. They may also have different physicochemical properties that affect the quality of the final solid dosage form [6]. A stable polymorph is commonly preferred in drug products. However, for some desirable applications, the meta-stable polymorph is usually considered, especially regarding its solubility, dissolution, and bioavailability, which affect the effectiveness of the drug [29, 50, 51]. Thus, tight supervision in a stringent regulatory environment regarding the polymorphism phenomenon is needed to control its

effect on bioequivalency among oral solid dosage forms on the market [1].

It is well-known that polymorphic transformation happens during the manufacturing process [11, 21, 25] or drug-excipient interactions [32, 33, 47]. Some potential processes in the development of oral solid dosage forms that induced the solid-state phase transition should be evaluated. Most potential processes causing polymorph transformation involve heat (e.g. drying, granulating) [15, 44, 49] and mechanical stress (e.g. mixing, grinding, sieving, and compression) [22, 25, 26, 34, 46]. Therefore, more attention should be devoted to the energy level during those processes to ensure that the desired polymorph has been formed during the phase transition. This is caused by unpredictable changes in the degree of transformation [31, 39]. Studies on polymorphic transformation kinetics

\* Corresponding author.

E-mail address: [ayodhna@gmail.com](mailto:ayodhna@gmail.com) (Y.W. Wardhana).<https://doi.org/10.1016/j.heliyon.2020.e03876>

Received 11 February 2020; Received in revised form 16 March 2020; Accepted 24 April 2020

2405-8440/© 2020 The Author(s). Published by Elsevier Ltd. This is an open access article under the CC BY-NC-ND license (<http://creativecommons.org/licenses/by-nc-nd/4.0/>).

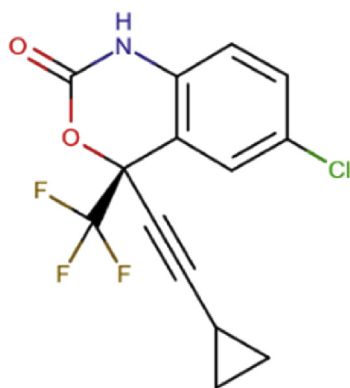


Figure 1. Structure of efavirenz.

and the mechanism driving interchangeable polymorphs are important to keep drugs as their pure forms.

Efavirenz (EFV) is a *non-nucleoside reverse transcriptase inhibitor* (NNRTI) used in the treatment of acquired immunodeficiency syndrome (AIDS); it is a first-choice drug for highly active antiretroviral therapy (HAART) [2]. Molecular EFV (Figure 1) with the chemical name (*S*)-6-chloro-4-(cyclopropylethynyl)-1,4-dihydro-4-(trifluoromethyl)-2(*H*)-3,1-benzoxazin-2-one was initially approved by the United States Food and Drug Administration (US FDA) in 1998 with no polymorphic forms. Recently, it has been reported to have 23 different forms, including amorphous and solvated forms [3, 7, 13, 14, 23, 35, 36, 37, 38, 40, 45]. Among these polymorphic forms, Form I (which can be purified using acetonitrile as the solvent) has the most stable form and has been widely chosen for production [13]. Many scientists have reported their work on improving the solubility, which is 3–9  $\mu\text{g}/\text{ml}$ , with a low intrinsic dissolution rate of 0.037  $\text{mg}/\text{cm}^2/\text{min}$  [4, 5, 10, 12, 16, 24, 42, 43, 45].

Many researchers have reported on thermodynamics and kinetics of EFV polymorphs [3, 18, 19], while others have reported molecular structural information on the polymorphs [8, 15, 27, 38]. The meta-stable forms present some advantages when manufactured into a product. However, polymorphic transformation kinetics and mechanistic studies on EFV as meta-stable forms are rare.

In this work, the effect of temperature (isothermal) and mechanical stress treatment (grinding) as manufacturing energy representatives for the transformation of form II to I were studied. As a preliminary study, characterisations of crystal morphology, vibrational spectra, thermal profiles and crystallographic properties were carried out to distinguish each polymorph.

Data collection under isothermal conditions and grinding was performed by Raman spectroscopy and powder diffraction as indispensable tools to give the complete information. Moreover, a full-pattern PXRD quantitative phase analysis (QPA) with Rietveld refinement analysis was performed for the quantification of the phase identification process. Afterwards, the determination of phase transformation was used to explain solid-state transformation kinetic and mechanistic behaviours.

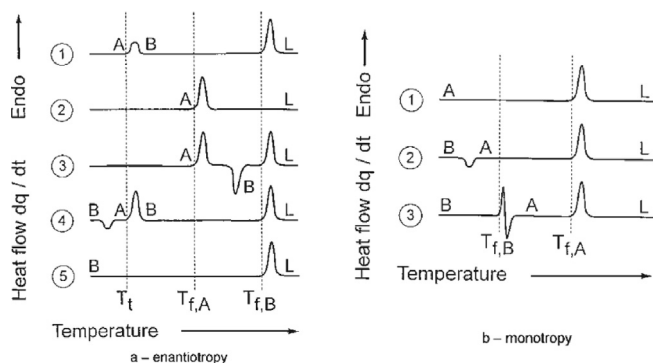


Figure 2. The differences in polymorphic transformation types [20].

## 2. Materials and methods

### 2.1. Raw materials and chemicals

The raw material of efavirenz (EFV, Batch No. EZ1670711, Hetero Labs Ltd., India) was purchased from PT. Kimia Farma Tbk., Indonesia. It was then recrystallised in organic solvents such as acetonitrile (form I) and n-hexane (form II) to give pure polymorphic forms. All solvents used were of analytical reagent grade without further purification.

### 2.2. Properties of polymorphs

#### 2.2.1. Polarisation light microscopy (PLM)

Crystal morphology was observed using an Olympus BX53 model ULH100-3 microscope. The sample was placed on a microscope slide and covered with a cover-slip.

#### 2.2.2. Scanning electron microscopy (SEM)

SEM images were obtained on a JEOL-SM (Japan), operated at an acceleration voltage of 15 kV and 12 mA. The samples were vacuum-coated with gold at a thickness of 10 nm before being placed in the aluminium holder.

#### 2.2.3. Fourier transform infrared (FTIR) spectroscopy

Fingerprints of the sample were recorded on a multi-scope spectrophotometer (IR Prestige-21 Shimadzu, Japan) by sealing the sample between two KBr plates using a hydraulic press at 200  $\text{kg}/\text{cm}^2$  for 15 s to form a disc. The spectrum for each sample was analysed in the spectral region of 300–4500  $\text{cm}^{-1}$  with a resolution of 4  $\text{cm}^{-1}$ .

#### 2.2.4. Raman spectroscopy

Raman spectra were collected using a Bruker-Senterra Micro-Raman Spectrometer with a diode laser system (785 nm, 100 mW) as the excitation source for spectrum recording at room temperature in the spectral region of 50–3500  $\text{cm}^{-1}$ .

#### 2.2.5. Differential scanning calorimetry (DSC)

The thermal profile of polymorphs was obtained using a Netzsch DSC 214 Polyma and an aluminium crucible. About 1–3 mg of the sample was measured under a dynamic nitrogen atmosphere and a heating rate of 10  $^{\circ}\text{C}/\text{min}$  in the temperature range from 30 to 250  $^{\circ}\text{C}$ . Before usage, the DSC device was calibrated with indium as a standard reference.

#### 2.2.6. Powder X-ray diffraction (PXRD)

The crystallinity of powders was investigated by an X-ray diffractometer (XPRT-PRO, PANalytical, The Netherlands) with  $\text{Cu-K}\alpha$  radiation. The diffractogram patterns were recorded under the following conditions: voltage 40 kV, 40 mA and fixed divergence slit using the configuration  $2\theta$  range: 5 $^{\circ}$  to 45 $^{\circ}$ , 0.02 step size, 0.8 s time per step. Care was taken to avoid phase transformations from unnecessary grinding or heating.

## 2.3. Polymorphic transition studies

### 2.3.1. Mechanical grinding

The transformation of polymorphs under mechanical force was assessed by grinding Form II for different times. The meta-stable sample (form II) were ground in a Retsch RM 100 at a steady rotation of 90 rpm for 10, 30, 60, 90, 120, 180 and 210 min.

### 2.3.2. Heating storage in an oven

Phase transition kinetics of EFV from Form II to Form I was studied under isothermal conditions at different temperatures and times. A sample of EFV Form II was kept in an oven (Mettler UN30, Germany) for different times (10–180 min). Each sample was at a temperature of 60

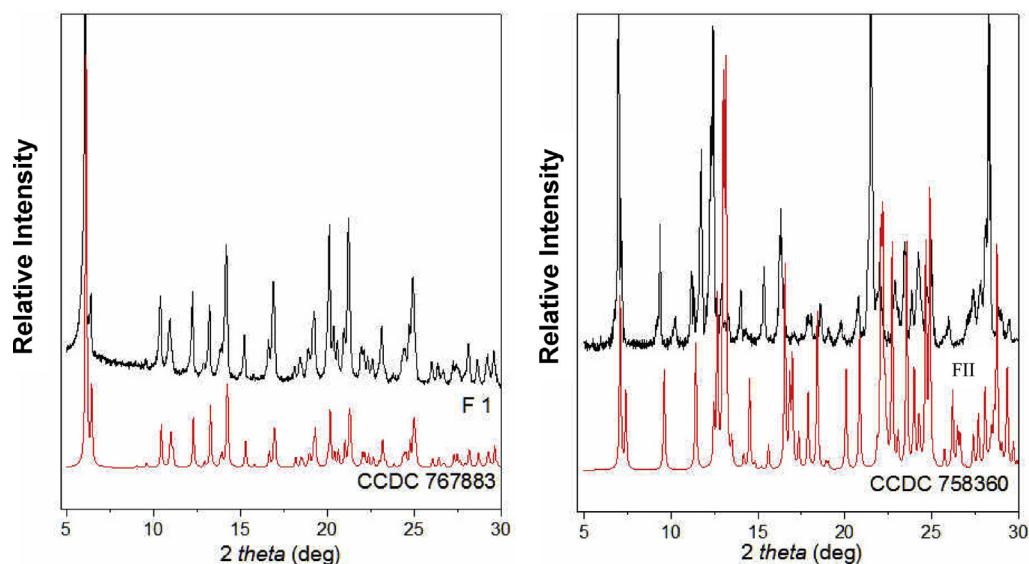


Figure 3. Comparison study from PXRD experimental data of EFV Form I (F1) and Form II (F2) with the calculated database.

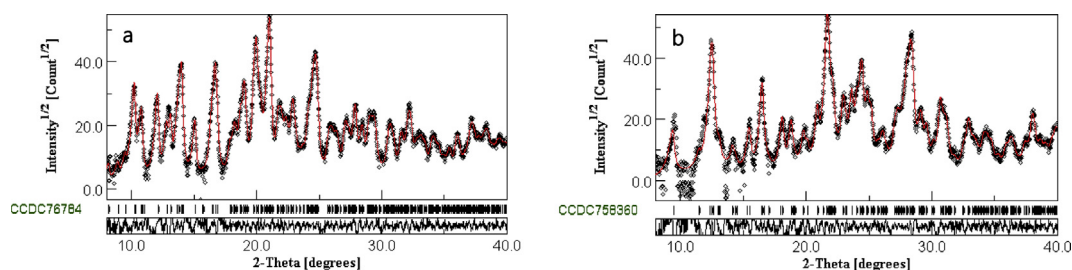


Figure 4. Rietveld refinement of experimental data with the CCDC database structure as a model for polymorphs (a) Form I and (b) Form II.

°C, 70 °C or 80 °C. The temperature of the polymorphic transition range was chosen based on the DSC analysis.

### 2.3.3. Data collection and analysis

All samples were analysed by PXRD. The quantification of the concomitant polymorphs during treatment was analysed based on Rietveld refinement with the Le Baile method using MAUD ver. 2.7 software.

## 3. Results and discussion

### 3.1. Properties of polymorphic solid-state forms

The polymorphic forms resulting from the purification of material with organic solvents were collected. EFV Form I was obtained from acetonitrile at 70 °C, whereas Form II was obtained from n-hexane at the

Table 1. Kinetic equations of common solid-state mechanisms [9, 21, 53].

Model	Equation/ $g(a)$	Mechanism
Nucleation growth (JMAEK model)		
J1	$k t = [-\ln(1 - a)]^{1/2}$	Avrami-Erofeyev, $n = 2$
J2	$k t = [-\ln(1 - a)]^{1/3}$	Avrami-Erofeyev, $n = 3$
J3	$k t = [-\ln(1 - a)]^{1/4}$	Avrami-Erofeyev, $n = 3$ (Random distribution)
J4	$k t = \ln[a/(1 - a)]$	Random nucleation (Prout-Tompkins)
Dimensional diffusion		
D1	$k t = a^2$	one-dimensional diffusion
D2	$k t = (1 - a) \ln(1 - a) + a$	two-dimensional diffusion
D3	$k t = 1 - 2/3 a - (1 - a)^{2/3}$	three-dimensional diffusion - Ginstling-Brounshtein
D4	$k t = [1 - (1 - a)^{1/3}]^2$	three-dimensional diffusion - Jander
Reaction-order ( $n$ )		
R1	$k t = -\ln(1 - a)$	first-order reaction
R2	$k t = 1/(1 - a) - 1$	second-order reaction
Geometrical contraction ( <i>phase boundary</i> )		
G1	$k t = a$	One-dimensional ( <i>zero-order reaction</i> )
G2	$k t = 1 - (1 - a)^{2/3}$	Two-dimensional (cylindrical symmetry)
G3	$k t = 1 - (1 - a)^{1/3}$	Three-dimensional (spherical symmetry)

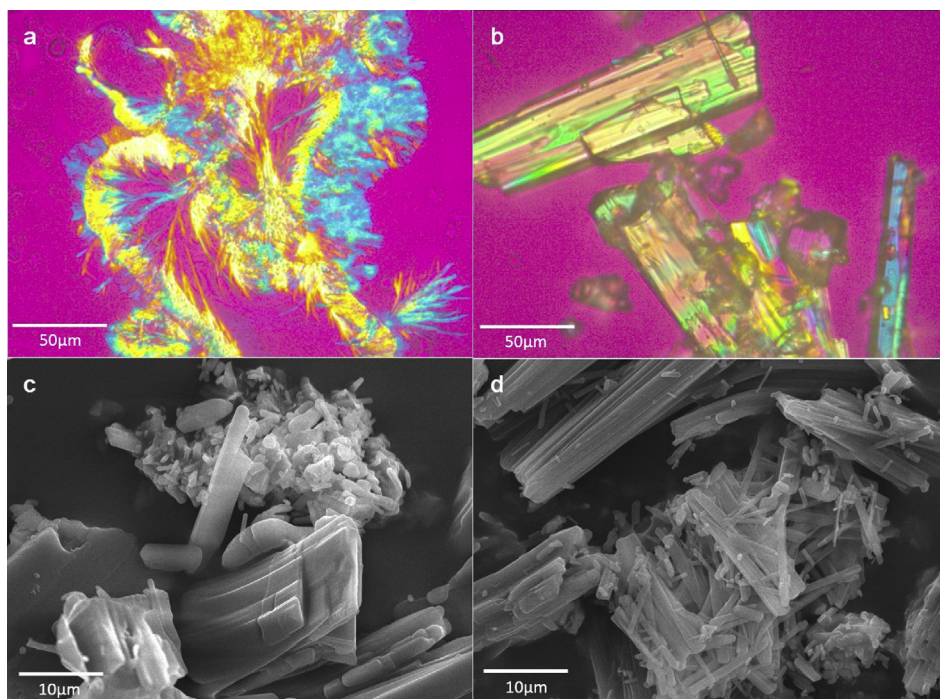


**Figure 5.** PLM Photomicrographs of efavirenz (EFV) polymorphs as reported in reference (52) with 400x magnification of (a) Form I, (b) Form II, and SEM picture of experimental purified sample of EFV with 2000x magnification of (c) Form I and (d) Form II.

same temperature. The resulting thermogram of purified polymorphs was compared with different types of polymorphic transformation thermograms as shown in Figure 2 [20].

The experimental diffractogram patterns collected were matched with those retrieved from the crystallographic structure file database of Cambridge Crystallographic Database Center (CCDC). It was found that the experimental data of Form I and II were (as published in Ref. 52) matched with CCDC no. 767883 and CCDC no. 758360 (shown in Figure 3). The result of the refinement of experimental data with a database structure from CCDC as a model is shown in Figure 4. Certain criteria were required to state that the fitting method used is a good fitting criterion. The agreement indexes were: for form I  $R_{wp} = 6.39\%$ ,  $R_{exp} = 3.84\%$ ,  $R_{Bragg} = 4.76\%$ , goodness of fit (GOF) = 1.66%, and for form II  $R_{wp} = 8.215\%$ ,  $R_{exp} = 3.61\%$ ,  $R_{Bragg} = 5.95\%$ , goodness of fit (GOF) = 2.27%. Those parameters were found to represent a good fit and used for quantitative phase analysis (QPA) to quantify concomitant polymorphs during treatment [28, 48]. By using multiphase refinement in fitting the diffractogram data treatment taken in the range 5–95 wt% with the database structures, the transformed fraction data were obtained. These data were then fitted to solid-state kinetic equations (Table 1). The

correlation coefficients ( $R^2$ ) derived from different fittings were used to evaluate the best-fit models ( $R^2 \approx 0.999$ ) as the mechanism of nucleation growth prediction [9, 21, 52].

It was found that recrystallisation revealed different crystal orientations when monitored by PLM at 400x magnification. The results were in line with those reported in a published article [52]. In order to get a clear picture, SEM at 2000x magnification was used as a comparator, as shown in Figure 5. By PLM observation, Form I showed birefringent crystalline areas with interference colours interspersed with grain boundaries, while those obtained by SEM revealed a clear looks crystalline shape which visually looked like a stack of plane boards. The observation of Form II using PLM showed stick-like crystals, while pictures obtained by SEM showed a columnar shape. This result shows that the differences were successfully achieved only by using different organic solvents in purification.

The difference in performance was due to molecular shifting around the functional group an in structural orientation, detectable by FTIR and Raman spectroscopy. The spectroscopy data from vibrational modes from each instrument should complement each other.

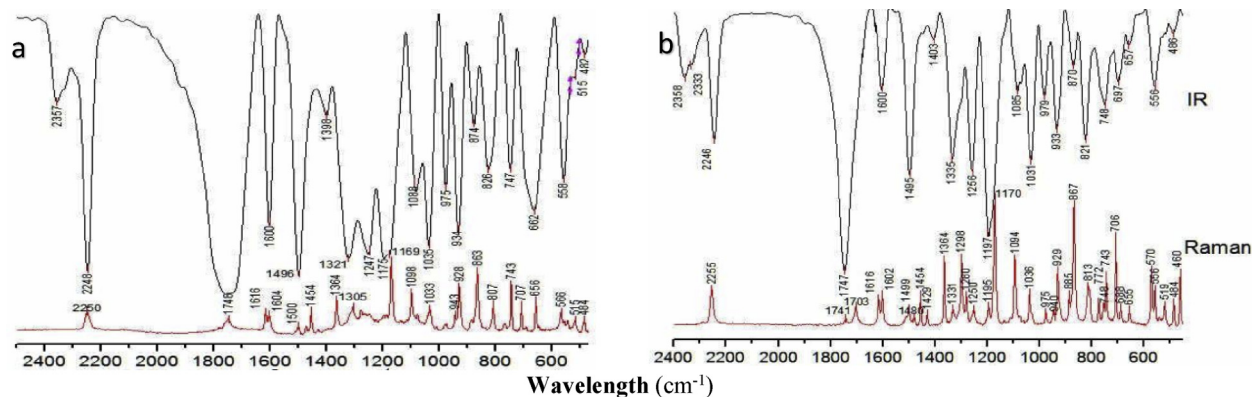


**Figure 6.** FTIR and Raman sapectrograph of efavirenz polymorphs as (a) Form I (b) Form II.

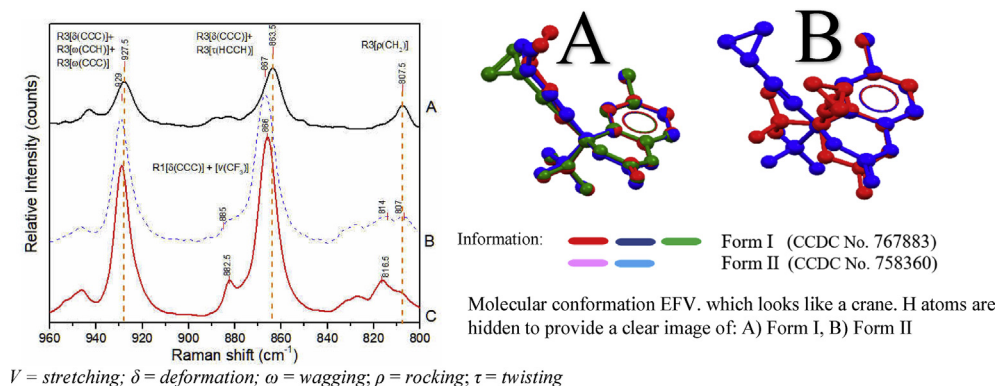


Figure 7. Raman spectrum of EFV polymorphic transformation from Form II to Form I.

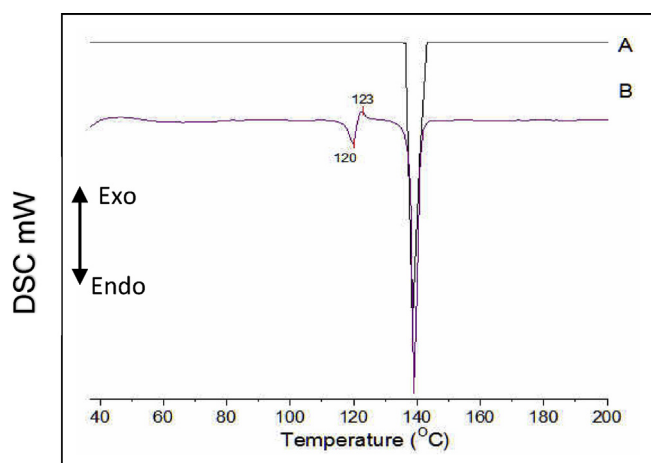


Figure 8. Thermogram of experimental EFV polymorphs as (A) Form I and (B) Form II.

In this report, the spectral region of wavelengths is shown in the range of  $500\text{--}2500\text{ cm}^{-1}$ . This range is enough to represent the

movement of deformations among the  $\text{CF}_3$ , cyclopropyl and benzoxazine groups in the EFV molecule, which have been reported by Mishra et al. [30]. As shown in Figure 6, Form I and II slightly differ in peak position and intensity at certain wavelengths in the IR and Raman spectra, but generally they have a similar pattern. The FTIR spectra of EFV has been reported by our group in a previous article [52]. Additional data by comparing the FTIR and Raman spectra allowed for a more comprehensive study into the shift of the polymorphs.

As shown in Figure 6, Form I has a high intensity in the IR spectra. In contrast, Form II showed intense and clear Raman spectra. This phenomenon can be explained by the presence of functional groups in the molecule of Form II as a centre of symmetry; thus, it can be seen as a Raman active vibration. Theoretically, symmetric and asymmetric stretch have a strong influence on polarisability. It can be concluded that Form II is more polarisable than Form I. According to a computational design by Riahi et. al [41] pairing the EFV modification molecules with DNA cancer, it was found that a high polarisability molecule may have great potential to be used as a drug of choice. This potency is due to the hydrogen bonding ability between the modified drug and cancer cell DNA, which has high polarisability [41].

At any wavelengths that represent the molecular vibrations of functional groups in this experiment, the range of wavelengths was between  $400\text{--}1200\text{ cm}^{-1}$ , which represents trifluoromethyl groups. The rocking

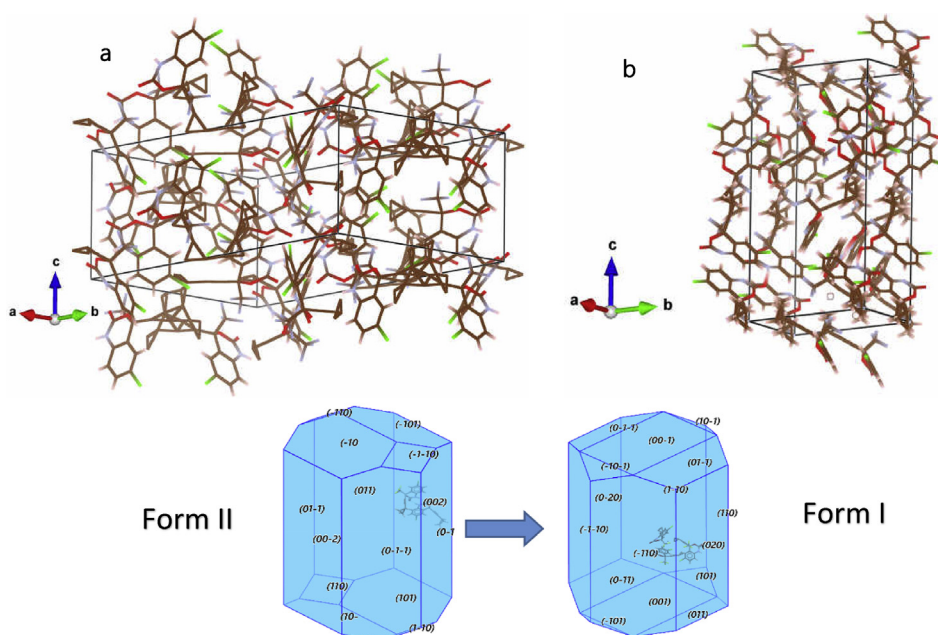
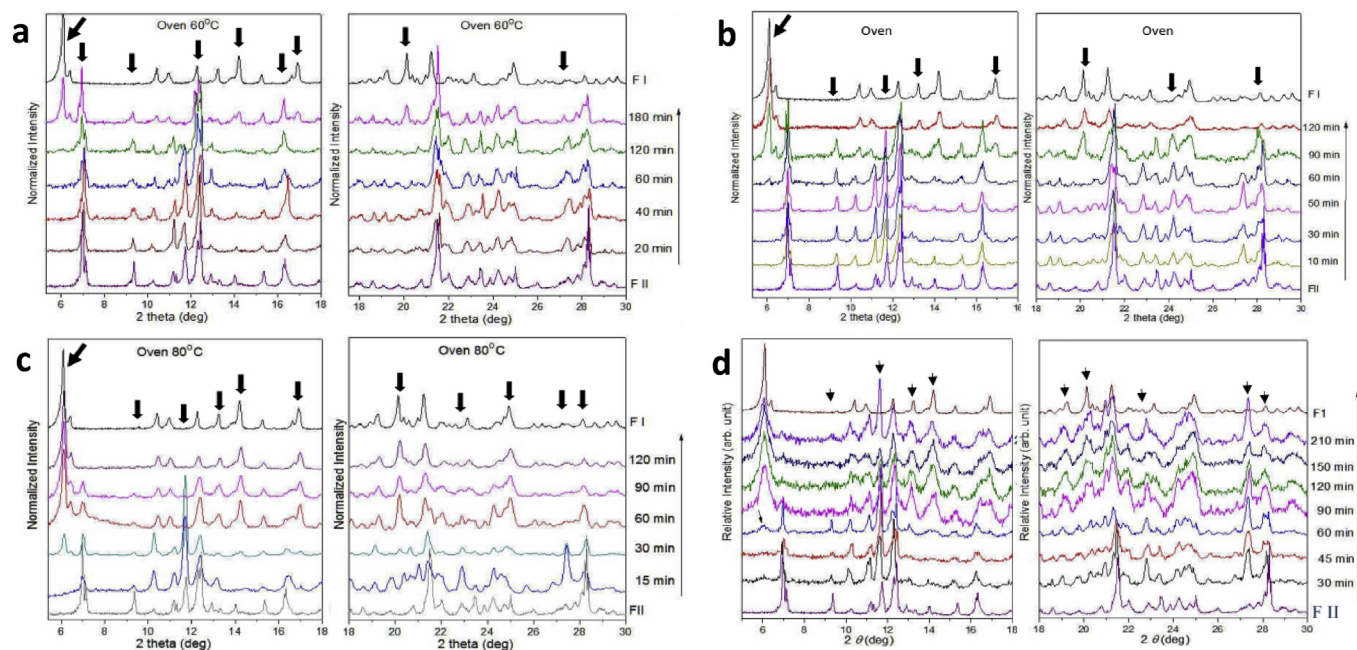


Figure 9. Three-dimensional packing of (a) Form I (CCDC no. 767884) and (b) Form II (CCDC no. 758360).



**Figure 10.** Diffractogram of the polymorphic transition from Form II to I stored in an oven at (a) 60 °C, (b) 70 °C, (c) 80 °C, and (d) after the grinding process.

mode of the  $\text{CF}_3$  band was represented at  $480\text{ cm}^{-1}$ . The symmetric stretching mode  $\nu_s(\text{CF}_3)$  was in the range of  $660\text{--}800\text{ cm}^{-1}$  while the asymmetric stretching  $\nu_a(\text{CF}_3)$  appeared in the range of  $1100\text{--}1200\text{ cm}^{-1}$ . The band at  $1400\text{ cm}^{-1}$  was from benzoxazine, oxazine and cyclopropyl ring group vibrations in different orientation. It also shows asymmetric stretch and deformation of the benzoxazine ring ( $\text{R1}_{[\nu_{\text{ring}}]} + \text{R1}_{[\delta(\text{CH})]}$ ). For oxazine ring, it is interpreted as ring deformation ( $\text{R2}_{[\delta(\text{NH})]}$ ) and in the cyclopropyl ring, the band represents plane CH bending. Meanwhile, the symmetric stretch of the benzoxazine ring ( $\text{R1}_{[\nu(\text{CC})]}$ ) band was defined at around  $1600\text{ cm}^{-1}$ . The band around  $1750\text{ cm}^{-1}$  was identified as oxazine ring stretch ( $\text{R2}_{[\nu(\text{CO})]}$ ). The band at around  $2300\text{ cm}^{-1}$  represented stretching mode of the alkyl chain ( $\nu_{\text{C}\equiv\text{C}}$ ).

In the Raman spectra, different peaks of bimorphism functional group movements were found (Figure 7). This result showed the movement of functional groups that result in the different crystal forms of the polymorphs. The movement of these functional groups causes conformational

differences such as the crane-like appearance as a result of modelling in Mercury ver. 3.8.

The difference in structural orientation makes the compounds divergent, leading to compounds with different energy levels. To study the energy levels of these compounds, the thermodynamic properties can be observed by employing DSC analysis. Not only does this assess the thermodynamic behaviour, but DSC thermograms can also give information about compound stability in nature [17]. According to Figure 8, Form II has two endothermic peaks and one exothermic peak, whereas Form I possessed only one endothermic peak. The thermograms show that Form II was transformed gradually with two endothermic peaks at  $120^\circ$  and  $138.6^\circ\text{C}$ . This profile was reported in our previous publication [52], but in the present report, further study of the pattern of polymorphic transformation is presented and discussed in comparison to literature data, as presented in Figure 2. By using this comparison, the mechanism of the polymorphic transformation of Form II can be

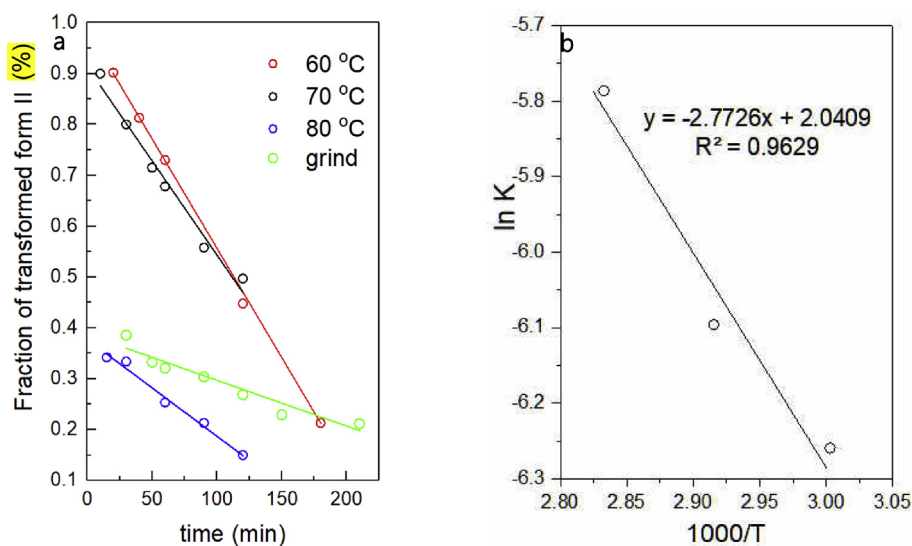


**Figure 11.** The polymorphic transition of Form II to Form I with (a) isothermal and grinding which quantified as the fraction of transformed Form II (%) vs. time (min) and (b) Arrhenius plot phase transition with three different temperature (60 °C, 70 °C, and 80 °C).

**Table 2.** Model fitting correlation coefficients ( $R^2$ ).

Model	oven heating at			Average $R^2$	Grinding 90 rpm
	60 °C	70 °C	80 °C		
J1	<b>0.999</b>	0.968	0.982	0.983	0.941
J2	0.995	0.950	0.984	0.976	0.937
J3	0.990	0.939	<b>0.985</b>	0.972	0.935
J4	0.987	0.925	0.982	0.965	0.941
D1	0.971	0.988	<b>0.986</b>	0.982	0.936
D2	0.947	0.983	0.982	0.971	0.947
D3	0.936	0.981	0.979	0.965	0.951
D4	0.967	0.986	<b>0.986</b>	0.979	0.925
R1	0.977	<b>0.995</b>	0.976	0.982	0.951
R2	0.901	<b>0.994</b>	0.936	0.944	<b>0.966</b>
G1	<b>0.998</b>	0.980	<b>0.985</b>	<b>0.988</b>	0.922
G2	0.996	0.989	<b>0.985</b>	<b>0.989</b>	0.938
G3	0.991	<b>0.991</b>	0.983	<b>0.988</b>	0.943

Bold values represents as correlation coefficients.

predicted. The study revealed that Form II has a monotropic style of transformation (exothermal solid-solid transition was observed). From the DSC thermogram, it could also be determined that the melting temperature of Form I ( $T_{m, I} = 138.6$  °C) was higher than that of Form II ( $T_{m, II} = 120$  °C) and the heat of fusion of Form I ( $\Delta H_{f, I} = 51$  J/g) was also higher than that of Form II ( $\Delta H_{f, II} = 7.5$  J/g). According to the heat-of-fusion rule, Forms I and II should be monotropically related. It also can be concluded that Form I is thermodynamically more stable and Form II exists in a meta-stable form.

From the PXRD diffractogram patterns in Figure 3, peaks distinguishing every phase were found. Form I showed peaks at  $2\theta$  5.89°, 10.24°, 10.74°, 12.06°, 13.06°, 14.04°, 15.08°, 16.74° and 19.06°, while Form II showed different distinct peaks at  $2\theta$  6.98°, 9.37°, 10.12°, 11.19°, 12.42°, 14.02°, 15.34° and 16.34°. According to the structural database, it can be assumed that they were in the same orthorhombic system, with a difference in space group of P21212 and P212121, respectively. Figure 9 shows that the difference in phases in the three-dimensional views of Form I and II are due to their landscape and portrait configurations. However, Form I revealed more molecules compared to that of Form II; thus, the denser bulk of Form I could be compared to Form II, which has a looser bulk. Analysing both crystals with BFDH law (Bravais-Friedel-Donnay-Harker Law) using Mercury ver. 3.8, it was found that those two forms of EFV polymorphs showed slightly different forms, which is in line with the PXRD results mentioned earlier. The BFDH results also revealed that Form II has a looser property than Form I, which agrees well with the PXRD data analysis in the current study (Figure 3).

### 3.2. Kinetic evaluation of EFV

It is well-known that there are two methods widely used for solid-state kinetic determinations, i.e. isothermal and non-isothermal methods. In this study, isothermal methods were used to evaluate the kinetics and mechanisms of the transformation of EFV from Form II to Form I. The experimental data are shown in Figure 10. Under isothermal kinetic analysis, wherein one variable was kept constant during the experiment (usually temperature, T), the amount of each kinetic parameter was specified simultaneously with the model fitting [53]. The mechanism and kinetics of transformation were assessed under different conditions: grinding time (15–210 min) and heating time (10–180 min) in an oven at three different storage temperatures (60 °C, 70 °C and 80 °C). The phase transition was quantified using an experimental diffractogram with Rietveld refinement in MAUD ver. 2.7 software (Figure 11a).

When the data of the transformed Form II fraction were plotted against time, a linear function with good correlation coefficients was obtained, providing a prediction of the equation to calculate polymorph transformation at a given time of the investigation, as shown in Table 2. This means that temperature variance gives different rates of heating, which can cause a different fraction of Form II crystals to transform into Form I. Assigning the fitting model, according to the  $R^2$  values shown in Table 2, is somehow tricky. The confirmation example can be given as the following: for heating at 60 °C, the values of  $R^2$  were 0.999 for the Avrami-Erofeyev (J1) and 0.998 of zero-order reaction (G1) models, respectively. Accordingly, at 70 °C, the heating spread evenly and a more ordered and homogeneous reaction was observed, such as one (R1) and second (R2) ordered, followed by the three-dimensional phase boundary (G3). By increasing the temperature to 80 °C, the heat was exposed and distributed evenly to every edge of the crystals providing, an increase in all the mechanisms except the ordered reaction mechanism.

The highest correlation was for dimensional diffusion (D) followed by phase boundary/geometry contraction (G). However, for the heat treatments, the correlation coefficient found to be the best fit for all heat treatments was the phase boundary in 2D or cylindrical symmetry (G2; 0.998). The highest correlation coefficient for mechanical treatment (grinding) was for the second-ordered mechanism (R2; 0.966). This means that, when performing heat treatment, nucleation is assumed to be dominantly diffuse by cylindrical symmetry growth, while when mechanical treatment is employed, the rate-limiting step follows a second-order reaction.

Figure 11b shows the decline in the fraction of Form II, which transformed to Form I with heat treatment. The temperature dependence of the rate constants based on the G2 mechanism (isothermal treatment) was analysed by the Arrhenius equation,

$$\ln k = -Ea / RT + \ln A$$

Using this equation, the energy activation during heating could be calculated; it should be around  $Ea = R \times \text{slope} = (8.314) \times (2.773) = 23.051$  kJ mol<sup>-1</sup>. From this equation, the half-life of Form II at ambient temperature ( $\pm 25$  °C) with the G2 mechanism was found to be approximately  $0.3/k = 0.3/(7 \times 10^{-4}) = 428.05$  min ( $\sim 7.1$  h).

## 4. Conclusions

Characterisation of EFV bimorphism as Forms I and II revealed that the polymorphs have different morphologies and different properties. According to the DSC results, Form II was predicted to have monotropy transition style, which agrees with the thermal profile in the literature

and the heat-of-fusion rule theory. The phase transformation between either Form II and Form I was investigated after isothermal and mechanical treatment, with a consideration for manufacturing purposes. The fitting results from the data with various solid-state kinetic equation models showed that the best correlation was found for the heating treatment, which showed the phase boundary reaction in a two-dimensional model (G2). It also concluded that the mechanical treatment (grinding) mechanism followed a second-order reaction (R2). Plotting the isothermal data with the Arrhenius equation revealed that activation energy was around 23.051 kJ mol<sup>-1</sup> with the half-life of Form II at ambient temperature around 428.05 min (~7.1 h).

## Declarations

### Author contribution statement

Y.W. Wardhana: Conceived and designed the experiments; Performed the experiments; Analyzed and interpreted the data; Contributed reagents, materials, analysis tools or data; Wrote the paper.

A. Hardian: Contributed reagents, materials, analysis tools or data.

A.Y. Chaerunnisa: Performed the experiments.

V. Suendo: Conceived and designed the experiments.

S.N. Soewandhi: Conceived and designed the experiments; Analyzed and interpreted the data.

### Funding statement

This research did not receive any specific grant from funding agencies in the public, commercial, or not-for-profit sectors.

### Competing interest statement

The authors declare no conflict of interest.

### Additional information

No additional information is available for this paper.

## Acknowledgements

The authors would like to acknowledge the supportive assistance from the School of Pharmacy, ITB and Faculty of Pharmacy, UNPAD. The authors are grateful for the collaborative efforts of Wisnu K.P., Jamelia A., Allin A.R.N., Fitria N, H. Hanifa N., Chrissel, Tazyinul Q.A., and Adelina K.R.

## References

- J.F. Bauer, Polymorphism – a critical consideration in pharmaceutical development, manufacturing, and stability, pharmaceutical solids, *J. Valid. Autumn.* (2008) 15–23.
- M. Bower, et al., The effect of HAART in 254 consecutive patients with AIDS-related Kaposi's sarcoma, *AIDS* 23 (2009) 1701–1706.
- R. Chadha, A. Saini, P. Arora, D.V.S. Jain, An insight into thermodynamic relationship between polymorphic forms of efavirenz, *J. Pharm. Pharmaceut. Sci.* 15 (2) (2011) 234–251.
- R. Chadha, A. Saini, P. Arora, S. Chanda, D.V.S. Jain, Cocrystals of efavirenz with selected cofomers: preparation and characterization, *Int. J. Pharm. Pharmaceut. Sci.* 4 (2) (2012) 244–250.
- D.A. Chiappetta, C. Hocht, C. Taira, A. Sosnik, Oral pharmacokinetics of the anti-HIV efavirenz encapsulated within polymeric micelles, *Biomaterials* 32 (2011) 2379–2387.
- N. Chieng, T. Rades, J. Aaltonen, An overview of recent studies on the analysis of pharmaceutical polymorphs, *J. Pharmaceut. Biomed. Anal.* 55 (2011) 618–644.
- W. Clarke, L.S. Crocker, J.L. Kukura, Process for the Crystallization of Reverse Transcriptase Inhibitor Using an Anti-solvent, Patent WO 98/33782, 1998, p. 29.
- S. Cuffini, R.A. Howie, E.R.T. Tiekink, J.L. Wardell, S.M.S.V. Wardell, (S)-6-Chloro-4-cyclopropyl ethynyl-4-trifluoromethyl-1H-3,1-benzoxazine-2(4H)-one, *Acta Crystallogr. E65* (2009) 3170–3171.
- P. Cui, Q. Yin, Y. Guo, J. Gong, Polymorphic crystallization and transformation of candesartan cilexetil, *Ind. Eng. Chem. Res.* 51 (2012) 12910–12916.
- M. da Costa, R. Seiceira, C. Rodrigues, C. Hoffmeister, L. Cabral, H.V.A. Rocha, Efavirenz dissolution enhancement I: Co-micronization, *Pharmaceutics* 5 (2013) 1–22.
- T.D. Davis, G.E. Peck, J.G. Stowell, K.R. Morris, S.R. Byrn, Modeling and monitoring of polymorphic transformation during the drying phase of wet granulation, *Pharm. Res.* 21 (5) (2004) 860–866.
- C.J. Destache, et al., Combination antiretroviral drugs in PLGA nanoparticle for HIV-1, *BMC Infect. Dis.* 9 (1) (2009) 198.
- J.A. Doney, Amorphous Efavirenz and the Production Thereof, Patent US 2007/0026073A1, 2007, p. 16.
- E. Dova, Polymorphic Forms of Efavirenz, WO 2008s/108630 A1, 2008.
- Y. Du, H. Zhang, J. Xue, W. Tang, H. Fang, Q. Zhang, Y. Li, Z. Hong, Vibrational spectroscopic study of poly-morphism and polymorphic transformation of the antiviral drug lamivudine, *Spectrochim. Acta A Mol. Biomol. Spectrosc.* 137 (2015) 1158–1163.
- T. Dutta, M. Garg, N.K. Jain, Targeting of efavirenz loaded tuftsin conjugated poly(propylene imine) dendrimers to HIV infected macrophages in vitro, *Eur. J. Pharmaceut. Sci.* 34 (2008) 181–189.
- C. Fandaruff, A.M. Araya-Sibaja, R.N. Pereira, C.R.D. Hoffmeister, H.V.A. Rocha, M.A.S. Silva, Thermal behaviour and decomposition kinetics of efavirenz under isothermal and non-isothermal conditions, *J. Therm. Anal. Calorim.* 115 (3) (2013) 2351–2356.
- C. Fandaruff, A.M. Araya-Sibaja, R.N. Pereira, S.L. Cuffini, C.E. Maduro de Campos, C.R.D. Hoffmeister, V.A. Rocha, Helvécio, M.A.S. Silva, Interaction and compatibility studies of efavirenz with pharmaceutical excipients, *J. Excipients Food Chem.* 5 (3) (2014) 152–160.
- B.D.L. Ferreira, B.C.R. Araujo, R.C.O. Sebastião, M.I. Yoshida, W.N. Mussel, S.L. Fialho, J. Barbosa, Kinetic study of anti-HIV drugs by thermal decomposition analysis: a multilayer artificial neural network propose, *J. Therm. Anal. Calorim.* 127 (2017) 577–585.
- D. Giron, Investigations of polymorphism and pseudo-polymorphism in pharmaceuticals by combined thermo-analytical techniques, *J. Therm. Anal. Calorim.* 64 (2001) 37–60.
- Z. Guo, M. Ma, T. Wang, D. Chang, T. Jiang, S. Wang, A kinetic study of the polymorphic transformation of nimodipine and indomethacin during high shear granulation, *AAPS PharmSciTech* 12 (2) (2011) 610–619.
- A. Hédoux, Y. Guinet, L. Paccou, F. Danèe, P. Derollez, Polymorphic transformation of anhydrous caffeine upon grinding and hydrostatic pressurizing analyzed by low-frequency Raman spectroscopy, *J. Pharmacol. Sci.* 102 (2) (2013) 162–170.
- H.C. Khanduri, A.K. Panda, Y. Kumar, Processes for the Preparation of Polymorphs of Efavirenz, WO 2006/030299A1, 2006.
- V.K. Kumar, A.M. Devi, D.V.R.N. Bhikshapathi, Development of solid self emulsifying drug delivery systems containing efavirenz: in vitro and in vivo evaluation, *Int. J. Pharm. Bio. Sci.* 4 (1) (2013) 869–882.
- Shan-Yang. Lin, Grinding and compression processes affecting the solid-state transition of famotidine polymorphs, *Asian J. Pharm. Sci.* 2 (5) (2007) 211–219.
- S.Y. Lin, W.T. Cheng, S.L. Wang, Thermodynamic and kinetic characterization of polymorphic transformation of famotidine during grinding, *Int. J. Pharmaceut.* 318 (2006) 86–91.
- S. Mahapatra, T.S. Thakur, S. Joseph, S. Varughese, G.R. Desiraju, New solid state forms of the anti-HIV drug efavirenz – conformational flexibility and high Z issues, *Cryst. Growth Des.* 10 (7) (2010) 3191–3202.
- L.B. McCusker, R.B. Von Dreele, D.E. Cox, D. Louer, P. Scardi, Rietveld refinement guidelines, *J. Appl. Crystallogr.* 32 (1999) 36–50.
- S. Miyazaki, T. Arita, R. Hori, K. Ito, Effect of polymorph-ism on the dissolution behavior and gastrointestinal absorption of chlortetracycline hydrochloride, *Chem. Pharm. Bull.* 22 (3) (1974) 638–642.
- S. Mishra, P. Tandon, A.P. Ayala, Study on the structure and vibrational spectra of efavirenz conformers using DFT: comparison to experimental data, *Spectrochim. Acta Part A* 88 (2012) 116–123.
- S.L. Morissette, Ö. Almarsson, M.L. Peterson, J.F. Remenar, M.J. Read, A.V. Lemmo, S. Ellis, M.J. Cima, C.R. Gardner, High-throughput crystallization: polymorphs, salts, co-crystals and solvates of pharmaceutical solids, *Adv. Drug Deliv. Rev.* 56 (2004) 275–300.
- R. Nair, S. Gonen, S.W. Hoag, Influence of polyethylene glycol and povidone on the polymorphic transformation and solubility of carbamazepine, *Int. J. Pharmaceut.* 240 (2002) 11–22.
- M. Otsuka, T. Ofusa, Y. Matsuda, Effect of binders on poly-morphic transformation kinetics of carbamazepine in aqueous solution, *Colloids Surf. B* 17 (2000) 145–152.
- Y. Otsuka, M. Yamamoto, H. Abe, M. Otsuka, Effects of polymorphic transformation on pharmaceutical properties of directly compressed tablets containing theophylline anhydrate bulk powder under high humidity, *Colloids Surf. B* 102 (2013) 931–936.
- Z. Perold, E. Swanepoel, M. Brits, Anomalous dissolution behavior of a novel amorphous form of efavirenz, *Am. J. PharmTech Res.* 2 (2) (2012) 272–292.
- L. Radesca, M. Maurin, S. Rabel, J. Moore, Crystalline Efavirenz, WO 99/64405, 1999.
- L. Radesca, M. Maurin, S. Rabel, J. Moore, Crystalline Efavirenz, US 6,673,372 B1, 2004.
- K. Ravikumar, B. Sridhar, Molecular and crystal structure of efavirenz, a potent and specific inhibitor of HIV-1 reverse transcriptase, and is monohydrate, *Mol. Cryst. Liq. Cryst.* 515 (2009) 190–198.

- [39] K. Raza, P. Kumar, S. Ratan, R. Malik, S. Arora, Poly-morphism: the phenomenon affecting the performance of drugs, *SOJ Pharm. Pharm. Sci.* 1 (2) (2014) 1–10.
- [40] B.P. Reddy, K. Rathnakar, R.R. Reddy, D.M. Reddy, K.S.C. Reddy, Novel Polymorphs of Efavirenz, US 2006/0235008, 2006, p. 6.
- [41] S. Riahi, S. Eynollahi, M.R. Ganjali, P. Norouzi, Computational studies on effects of efavirenz as an anticancer drug on DNA: application in drug design, *Int. J. Electrochem. Sci.* 5 (2010) 815–827.
- [42] S. Sathigari, et al., Physicochemical characterization of efavirenz-cyclodextrin inclusion complexes, *AAPS PharmSciTech* 10 (2009) 81–87.
- [43] S.K. Sathigari, V.D. Radhakrishnan, V.A. Davis, D.L. Parsons, R.J. Babu, Amorphous-state characterization of efavirenz-polymer hot-melt extrusion system for dissolution enhancement, *J. Pharmacol. Sci.* 101 (9) (2012) 3456–3464.
- [44] E.G. Shami, P.D. Bernardo, E.S. Rattie, L.J. Ravin, Kinetics of polymorphic transformation of sulfathiazole form I, *J. Pharmacol. Sci.* 61 (8) (1972) 1318–1320.
- [45] R. Sharma, H.K. Bhushan, R.C. Aryan, N. Singh, B. Pandya, Y. Kumar, Polymorphic Forms of Efavirenz and Processes for Their Preparation, WO 2006/040643 A2, 2006.
- [46] S.J. Smith, M.M. Bishop, J.M. Montgomery, T.P. Hamilton, Y.K. Vohra, Polymorphism in paracetamol: evidence of additional forms IV and V at high pressure, *J. Phys. Chem. A* 118 (2014) 6068–6077.
- [47] Y. Sun, L. Zhu, T. Wu, T. Cai, E.M. Gunn, L. Yu, Stability of amorphous pharmaceutical solids: crystal growth mechanisms and effect of polymer additives, *AAPS J.* 14 (3) (2012) 380–388.
- [48] B.H. Toby, R factors in Rietveld analysis: how good is good enough? *Powder Diff.* 21 (1) (2006) 67–70.
- [49] Ts. Umeda, N. Ohnishi, T. Yokoyama, Ts. Kuroda, Y. Kita, K. Kuroda, E. Tatsumi, Y. Matsuda, A kinetic study on the isothermal transition of polymorphic forms of tolbutamide and mefenamic acid in the solid state at high temperatures, *Chem. Pharm. Bull.* 33 (5) (1985) 2073–2078.
- [50] K. Urakami, Y. Shono, A. Higashi, K. Umemoto, M. Godo, A novel method for estimation of transition temperature for polymorphic pairs in pharmaceuticals using heat of solution and solubility data, *Chem. Pharm. Bull.* 50 (2) (2002) 263–267.
- [51] A. Watanabe, Y. Yamaoka, K. Takada, Crystal habits and dissolution behavior of aspirin, *Chem. Pharm. Bull.* 30 (8) (1982) 2958–2963.
- [52] Y.W. Wardhana, S.N. Soewandhi, S. Wikarsa, V. Suendo, Polymorphic properties and dissolution profile of efavirenz due to solvents recrystallization, *Pak. J. Pharm. Sci.* 32 (3) (2019) 981–986.
- [53] Q. Zhang, L. Jiang, X. Meng, Thermodynamic and kinetic investigation of agomelatine polymorph transformation, *Pharm. Dev. Technol.* 21 (2) (2016) 196–203.